Plant Physiology and Biochemistry 121 (2017) 216–225

Contents lists available at ScienceDirect

Plant Physiology and Biochemistry

journal homepage: www.elsevier.com/locate/plaphy

Research article

Protective role of biosynthesized silver nanoparticles against early blight disease in *Solanum lycopersicum*

Madhuree Kumari[a,b], Shipra Pandey[a,b], Arpita Bhattacharya[a,b], Aradhana Mishra[a,b,*], C.S. Nautiyal[a]

[a] Department of Plant Microbe Interactions, CSIR-NBRI, Lucknow, 226001, U.P, India
[b] Academy of Scientific and Innovative Research (AcSIR), Ghaziabad, 201002, U.P, India

ARTICLE INFO

Keywords:
Tomato
Alternaria solani
Silver nanoparticles
Tripartite interaction
Native microflora

ABSTRACT

Tomato suffers a huge loss every year because of early blight disease. This study focuses on efficient inhibition of *Alternaria solani,* the causative agent of early blight disease in tomato *in vitro* and *in vivo*. Foliar spray of 5 μg/mL of biosynthesized silver nanoparticles in *A. solani* infected plants resulted in significant increase of 32.58% in fresh weight and 23.52% in total chlorophyll content of tomato as compared to *A. solani* infected plants. A decrease of 48.57, 30, 39.59 and 28.57% was observed in fungal spore count, lipid peroxidation, proline content and superoxide dismutase respectively in infected tomato plants after treatment with synthesized silver nanoparticles as compared to *A. solani* infected plants. No significant variation in terms of soil pH, cultured population, carbon source utilization pattern and soil enzymes including dehydrogenase, urease, protenase and β-glucosidase was observed after foliar spray of nanoparticles. It was revealed that direct killing of pathogens, increased photosynthetic efficiencies, increased plant resistance and decrease in stress parameters and stress enzymes are the mechanisms employed by plants and nanoparticles simultaneously to combat the biotic stress. Biosynthesized silver nanoparticles bear the potential to revolutionize plant disease management, though the molecular aspects of increased resistance must be looked upon.

1. Introduction

In a very short span of time, nanotechnology has occupied a prominent position to human welfare by its multifactorial roles (Javed et al., 2017; Kumari et al., 2017a). It has revolutionized every aspect of biomedical, sensing, engineering and catalytic applications (Mishra et al., 2014; Wang et al., 2015; Kumari et al., 2016), however their uses in agriculture are still in nascent stage.

Silver nanoparticles are known for their antifungal role since a long time, but their uses to control phytopathogens in field conditions has been restricted owing to dearth of knowledge regarding their effect on plant system and native soil microflora. Some reports describe antifungal and antibacterial activities of silver nanoparticles in field and greenhouse conditions against plant pathogens, but the effects of particles on plant and soil microflora during tripartite interaction of plant-pathogen and nanoparticles is unknown (Mishra et al., 2014; Ocsoy et al., 2013). Manipulation in the route of silver nanoparticles synthesis, their structural properties and surface coating are some of the methods which are being used for enhancing the antimicrobial activities of silver nanoparticles (Jamshidi and Ghanati, 2016; Kumari et al., 2017b).

Tomato (*Solanum lycopersicum* Mill.) is one of the important vegetable crops grown worldwide contributing a substantial share to productivity of fields and economic benefits to farmers (Khan et al., 2012; Dixit et al., 2016). Early blight, caused by *Alternaria solani* is one of the most devastating diseases affecting tomato, decreasing its productivity by 80% (Khan et al., 2012). Practices to overcome this deadly disease includes use of resistant varieties, chemical fungicide application and induction of systemic acquired resistance in plants, but climate change and emergence of resistant pathogens have restricted the use of traditional methods (Khan et al., 2012; Ocsoy et al., 2013). Silver nanoparticles possess multiple modes of actions (Ocsoy et al., 2013) which make it difficult for pathogen to acquire resistance. In this study, spherical biogenic silver nanoparticles (2–5 nm) were used after optimizing the synthesis conditions of *Trichoderma viride* (Kumari et al., 2017c). These biosynthesized nanoparticles have antimicrobial properties of both, of silver nanoparticles and secondary metabolites of *T. viride,* acquired during surface coating of particles (Kumari et al., 2017b).

Interaction of nanoparticles with plants during various conditions has revealed many new facts about plants adaptation and behaviour (Tripathi et al., 2015). Tripathi et al. (2017) has demonstrated the synergistic effect of plant and silicon nanoparticles during amelioration of UV-B stress and heavy metal stress, however effect of silver

* Corresponding author. Division of Plant Microbe Interactions, CSIR- NBRI, Rana Pratap Marg, Lucknow, 226 001, India.
E-mail address: mishramyco@yahoo.com (A. Mishra).

https://doi.org/10.1016/j.plaphy.2017.11.004
Received 6 September 2017; Received in revised form 8 November 2017; Accepted 8 November 2017
Available online 10 November 2017

nanoparticles application on resistance of plants during biotic stress has not been explored yet.

The fate of plant-pathogen interaction depends upon the strategies employed by plant to combat the pathogen attack. Several mechanisms including increase in phenolics and ascorbic acid, callose depositions and generation of antioxidants are employed to strengthen the plant defence machinery whereas; generation of reactive oxygen species (ROS) is employed by the pathogen to establish an infection. Induction of antioxidant enzymes including superoxide dismutase, catalase, peroxidase, polyphenol oxidase, phenylalanine ammonia lyase and guaiacol peroxidase also plays an important role to ameliorate stress by plant systems (Tripathi et al., 2017).

There is a need to investigate the effects of nanomaterials when they are being used in agriculture. Negative or negligible effects of nanoparticles in a concentration and route of administration dependent manner have been reported in literature (Wang et al., 2016). The behaviour of particles entering into soil via plant transport during application of nanoparticles on plant also needs a proper investigation.

Present study demonstrates the synergistic effects of biosynthesized silver nanoparticles and elevated plant resistance in amelioration of early blight disease of tomato. The impact of said nanoparticles on native microflora of soil was also assessed during the interaction of plant- *A. solani* and biosynthesized silver nanoparticles.

2. Materials and methods

2.1. Materials

Spherical silver nanoparticles (2–5 nm) were synthesized from cell free extract of *Trichoderma viride* (MTCC 5661) as described by Kumari et al. (2017c) and concentration was adjusted to 0.02 mg/mL before use. Particles were filtered through 0.22 μ syringe millipore filters and sonicated for 2 min before use (Kumari et al., 2017d). Media were purchased from Himedia lab, Mumbai, India. All other chemicals and reagents were of highest purity analytical grade.

2.2. Antagonistic effect of biosynthesized silver nanoparticles (SNP) against A. solani

For antifungal activity, potato dextrose broth (PDB) was supplemented with different concentrations of nanoparticles with 5, 10, 20 and 25% SNP of concentration 0.02 mg/mL. A bid of pathogenic fungi was inoculated in above prepared broth. Reduction in dry weight and spore count was calculated after 1st, 2nd, 3rd, 5th and 7th day of inoculation. Dry weight and spore reduction was also calculated with broth supplemented with silver nitrate and *T. viride* cell free filtrate to observe the effect of SNP in comparison to precursor salt and reducing agent.

2.3. Detached leaf assay

Fifteen days old tomato leaves were washed with ultrapure water and surface sterilized by 0.4% sodium hypochlorite solution for 60s, followed by rinsing with sterile water for 5 times. Leaves were dipped in 5 mL (5 μg/mL) silver nanoparticles based upon the results of broth assay, for 30 min and placed on 0.8% agar plates while leaves dipped in sterile water served as control. Spore suspension (10^5spores/mL) of *A. solani* was prepared in 1% gelatin and spotted on leaves (3spots/leaf) with 10 μL of spore suspension. Reduction in disease severity was measured by visual observation and the reduction in spore count as compared to control leaves.

2.4. Greenhouse studies

The field experiments were set up following the method of Dixit et al. (2016) with some modifications. Seeds were sown in seedling trays in garden soil and incubated in a growth chamber at 25 °C. After one week of germination, the seedlings were transferred to greenhouse (28°C/22 °C day/night) and grown under natural illumination. Four weeks old tomato seedlings were transplanted into plastic pots containing mixture of soil: sand: vermiculite in 1:1:1 ratio and following treatments were given. 1. Control (Con) 2. Plants treated with biogenic silver nanoparticles (SNP) 3. Plants infected with *A. solani* (AS alone) 4. Plants with both silver nanoparticles and challenged with *A. solani* (AS + SNP). Control plants were sprayed with 1% gelatin, while SNP and AS + SNP treatments were sprayed with the biogenic nanoparticles of concentration 5 μg/mL until runoff. Two hours after treatment, AS and AS + SNP treatments were inoculated with spore suspension of *A. solani* (10^5spores/mL). Plants were bagged with a transparent plastic bag and kept for 48 h. After 10 days of infection, plant was observed for disease symptoms and leaf samples were harvested immediately in liquid nitrogen and kept in −80 °C till further analysis.

2.5. Disease parameters assessment

Ten days post infection, samples were collected for counting number of lesions/leaf, no of spores/leaf, chlorophyll content (Arnon, 1949) and fresh and dry weight of leaves.

2.5.1. Stress parameters assessment

2.5.1.1. Proline. Free proline content in the leaves was determined by method of Bates et al. (1973). Briefly, 500 mg of leaves samples were homogenized in 5 ml of sulphosalycylic acid, 2 mL of which was mixed with equal volume of glacial acetic acid and ninhydrin reagent. The reaction mixture was boiled in water bath at 100 °C for 30 min and allowed to cool followed by addition of 6 mL of toluene and mixed properly. The chromophore containing toluene was separated and absorbance read at 520 nm in spectrophotometer against toluene blank.

2.5.1.2. Lipid peroxidation. Lipid peroxidation (LPX) was determined by estimating content of thiobarbituric acid reactive substances (TBARS) (Heath and Packer, 1968) with some modification. 500 mg of leaves were homogenized in 5 ml of 0.1% TCA and centrifuged at 10,000 × g for 5 min. For every 1 mL of aliquot, 4 ml of 20% TCA containing 0.5% thiobarbituric acid was added and heated at 95 °C for 30 min and then cooled quickly on ice bath. The absorbance of supernatant was taken at 532 and 600 nm. The non-specific absorbance at 600 nm was subtracted from the absorbance at 532 nm. The concentration of TBARS was calculated by using the extinction coefficient of 155 mM^{-1} cm^{-1}.

2.6. Determination of antioxidant activities

2.6.1. Enzymatic parameters

Activities of antioxidant enzymes were measured following the protocols of Mishra et al. (2006) with some modifications. 500 mg of leaves was homogenized in 100 mM potassium phosphate buffer (pH 7.0) containing 0.1 mMEDTA and 1% polyvinylpyrrolidone (w/v) at 4 °C. Homogenate was centrifuged at 15,000 × g for 15 min at 4 °C. Aliquots of supernatant were prepared and stored at −80 °C to measure the activities of enzymes. The protein content in the supernatants was measured by Bradford method (Bradford, 1976).

2.6.1.1. Superoxide dismutase (EC 1.15.1.1). The SOD activity in leaves was measured by the protocol of Beauchamp and Fridovich (1971). The 3 mL reaction mixture was prepared containing 40 mM phosphate buffer (pH 7.8), 13 mM methionine, 75 μM nitrobluetetrazolium, 2 μM riboflavin, 0.1 mM EDTA and 100 μL of enzyme extract. Riboflavin was added at the end. The test tubes were placed 30 cm below light source consisting of 15-W fluorescent lamp. Tubes containing protein kept in dark served as blank while the tube without the enzyme and kept in light served as control. The absorbance of the solution was measured at 560 nm. One unit of activity is the amount of protein required to inhibit 50% of initial reduction of NBT under light.

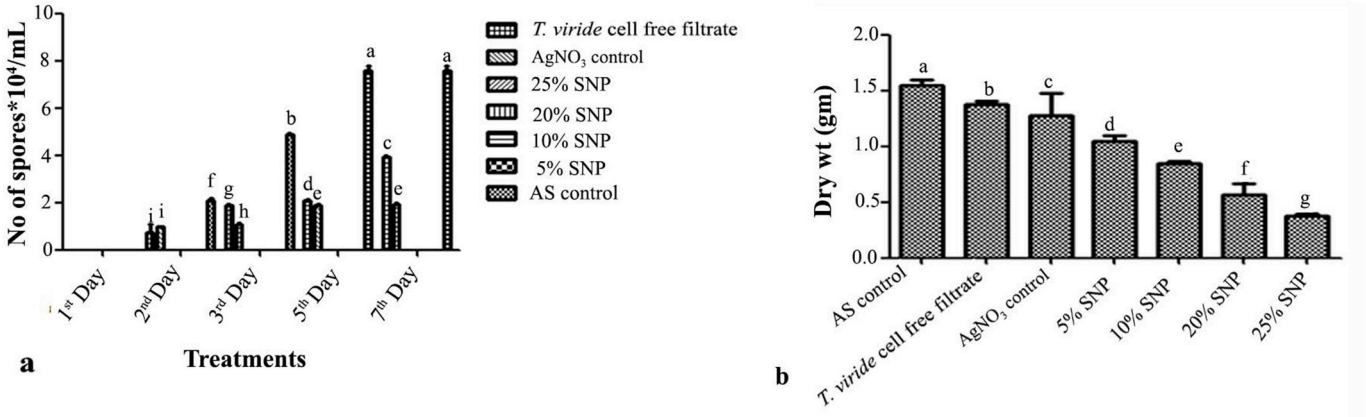

Fig. 1. *In vitro* anti fungal activity of SNP against *A. solani*: **(a)** Broth assay: Reduction in spore count **(b)** Reduction in dry weight. Values are the means of three replicates. Means sharing different alphabets "a", "b" differ significantly from each other at $p \leq 0.05$.

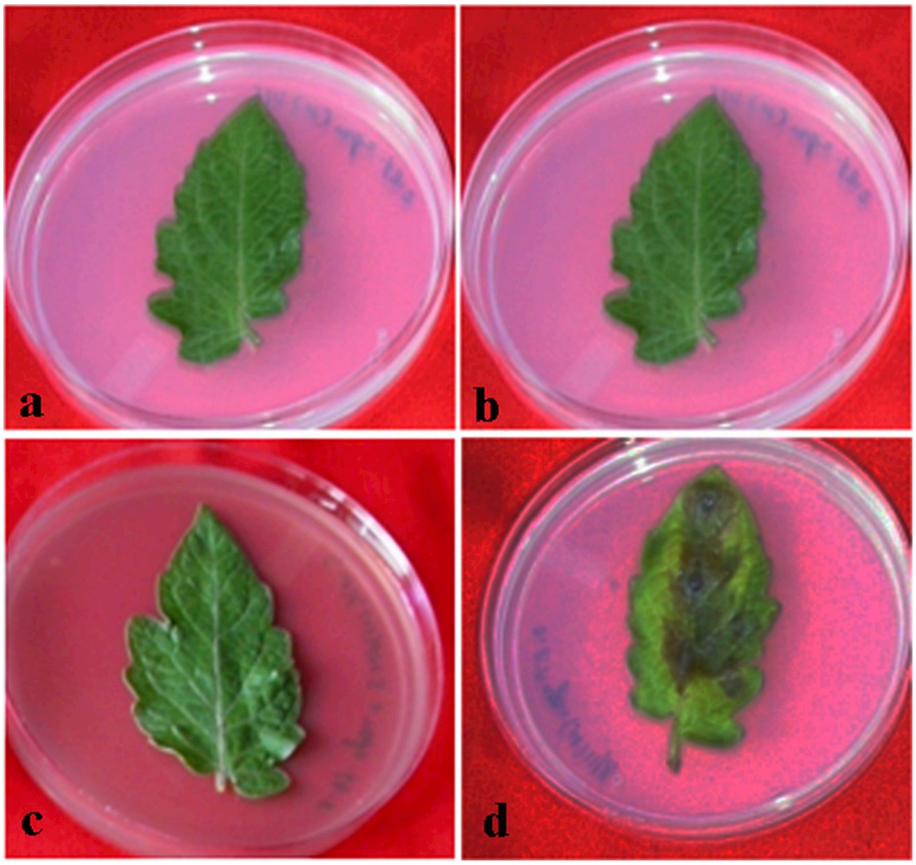

Fig. 2. Detached tomato leaf assay: **(a)** healthy leaf treated with gelatine **(b)** healthy leaf treated with SNP **(c)** *A. solani* infected leaf treated with SNP **(d)** *A. solani* infected leaf.

2.6.1.2. Ascorbate peroxidease (EC 1.11.1.11). APX activity was measured by the protocol of Mishra et al. (2006) with some modifications. Briefly, 3 mL reaction mixture contained 50 mM phosphate buffer (pH 7.0), 0.1 mM H_2O_2, 0.5 mM sodium ascorbate, 0.1 mM EDTA and enzyme extract. The change in absorbance was monitored at 290 nm and enzyme activity was expressed as u/min/mg of protein.

2.6.1.3. Guaiacol peroxidase (EC 1.11.1.7). GoPX activity was measured according to the method of Hemeda and Klein (1990). Reaction mixture of 10 mL was prepared by adding 1 mL of 1% guaiacol (v/v), 1 mL of 0.3% H_2O_2 and 8 ml of 50 mM phosphate buffer (pH 6.6). 100 µL of enzyme extract was added to reaction mixture with a final volume of 3 mL. The increase in absorbance due to oxidation of guaiacol (extinction coefficient 26.6 mM^{-1} cm^{-1}) was measured at 470 nm. Enzyme activity was expressed as u/min/mg of protein.

2.6.1.4. Polyphenol oxidase (EC 1.14.18.1). To assay PPO, 200 µL of enzyme extract was mixed with 700 µL of homogenization buffer containing 50 mM sodium phosphate buffer (pH 7.0), 20 mM H_2O_2. The rate of increase in absorbance at 420 nm for 1 min was recorded after the addition of 100 µL of 0.2 mM catechol and activity was expressed as Δ OD/min/g of protein (Lavania et al., 2006).

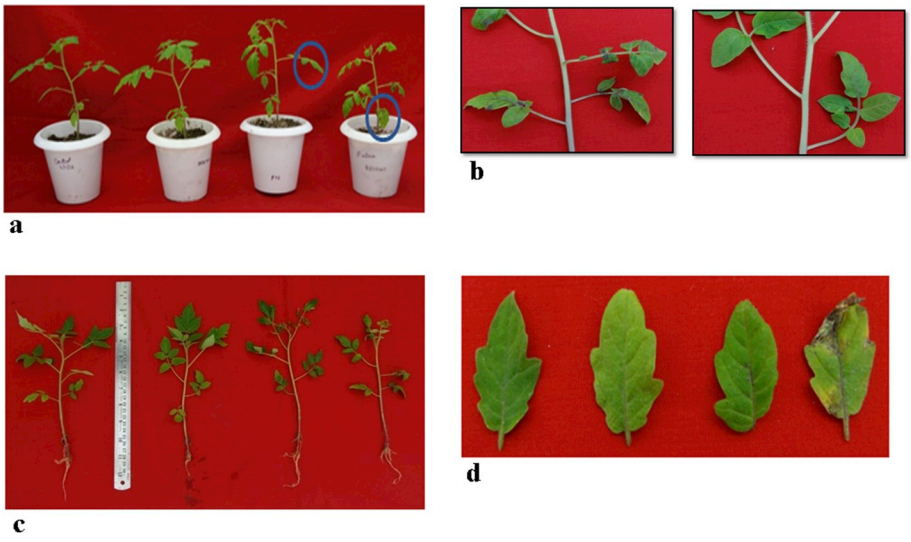

Fig. 3. *In vivo* anti fungal activity of SNP against *A. solani*:**(a)** Pots in sequence of control, SNP, AS + SNP and AS alone respectively **(b)** Enlarged view of AS infected and AS + SNP leaves **(c)** plant growth parameter of control, SNP, AS + SNP and AS alone plant respectively **(d)** single leaf with control, SNP, AS + SNP and AS alone treatments respectively.

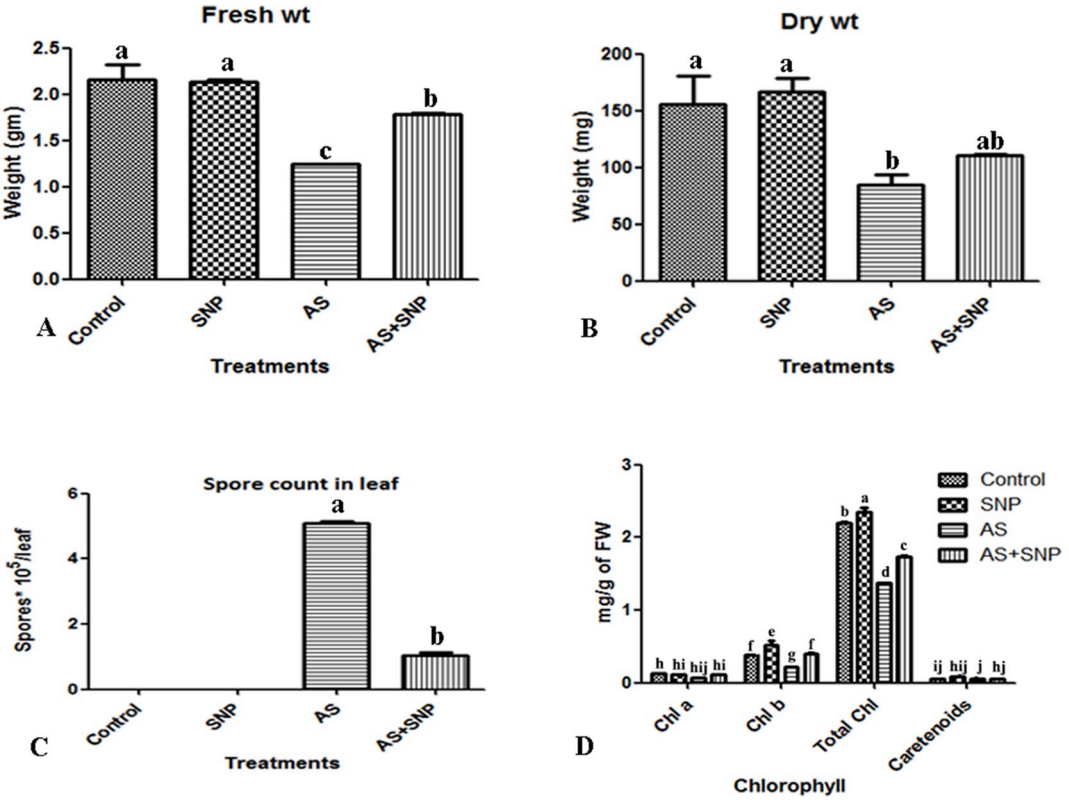

Fig. 4. Plant disease parameters: **(a)** Increase in fresh weight **(b)** Increase in dry weight **(c)** Decrease in spore count of *A. solani* per leaf **(d)** Increase in chlorophyll content. Values are the means of three replicates. Means sharing different alphabets "a", "b" differ significantly from each other at $p \leq 0.05$.

2.6.1.5. Phenylalanine ammonia lyase (EC 4.3.1.24). Phenylalanine ammonia lyase (PAL) activity was measured according to the method of Lavania et al. (2006) with some modifications. 100 µL leaf extract prepared for enzymatic assay as described earlier was mixed with 900 µL of 6 µM L-phenylalanine and 0.5 M Tris-HCl buffer solution. The mixture was placed in a water bath at 37 °C for 70 min. PAL activity was determined spectrophotometrically at a wavelength of 290 nm ultraviolet (UV) light. Cinnamic acid was used as the standard, and the results were expressed as µM TCA/g of protein.

2.6.2. Non enzymatic parameters

2.6.2.1. Total phenolics. Total phenolic content in plants was determined using Folin-Ciocalteu's reagent (Mallick and Singh, 1980). 50 mg of fresh plant material was crushed in 5 mL of 50% methanol. The homogenate was filtered through whattman filter paper. The filtrate was allowed to evaporate to obtain a residue. 5 mL of DW., 0.5 mL of Folin and Ciocalteu's Phenol reagent and 1 mL of 20% sodium carbonate were added to the residue. The mixture was vortexed and then incubated at room temperature for 20 min. OD was measured at 720 nm against reagent blank and results were expressed as ppm of gallic acid/gram of FW.

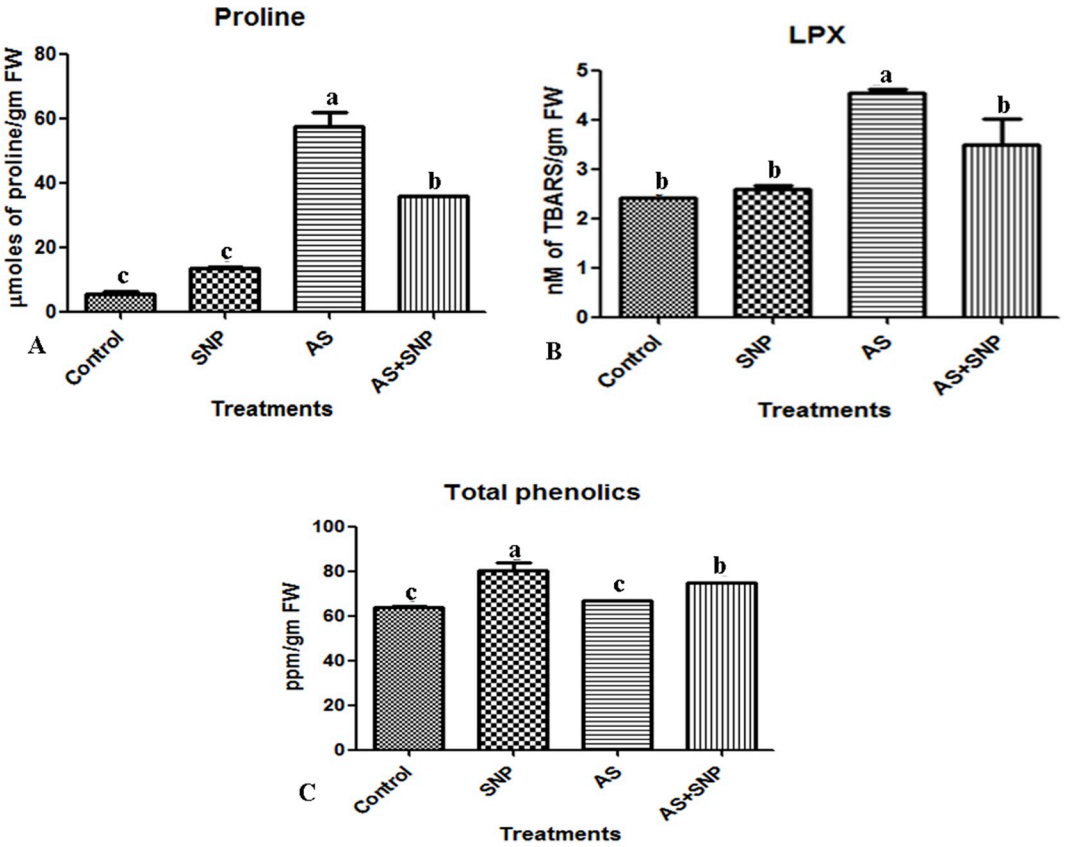

Fig. 5. Assessment of stress parameters: **(a)** Proline **(b)** lipid peroxidation **(c)** total phenolics. Values are the means of three replicates. Means sharing different alphabets "a", "b" differ significantly from each other at $p \leq 0.05$.

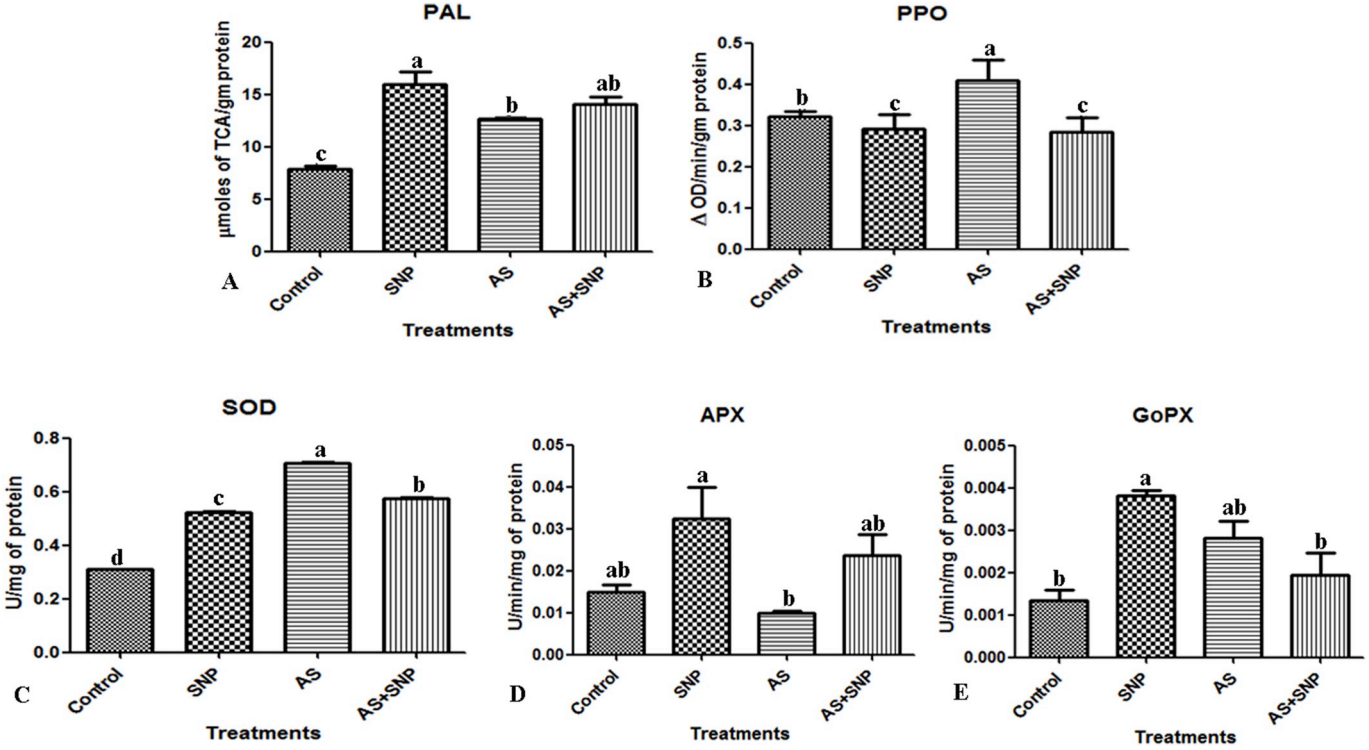

Fig. 6. Determination of antioxidative enzyme activities **(a)** Phenylalanine ammonia lyase (PAL) **(b)** Polyphenol oxidase (PPO) **(c)** Superoxide dismutase (SOD) **(d)** ascorbate peroxidease (APX) **(e)** Guaiacol peroxidise (GoPX). Values are the means of three replicates. Means sharing different alphabets "a", "b" differ significantly from each other at $p \leq 0.05$.

Table 1
pH and EC of soil after application of biosynthesized silver nanoparticles on tomato leaves. Values are the means of three replicates. Means sharing different alphabets "a", "b" differ significantly from each other at $p \leq 0.05$.

Treatment	pH	EC (μS/cm)
Control	8.0[a]	49.8[b]
SNP	8.08[a]	48.4[c]
AS	8.0[a]	117.3[a]
AS + SNP	8.01[a]	41.7[d]

Table 2
Heterogeneous microbial population in soil after application of biosynthesized silver nanoparticles on tomato leaves. Values are the means of three replicates. Means sharing different alphabets "a", "b" differ significantly from each other at $p \leq 0.05$.

Treatment	Bacteria (log_{10} CFU/mL)	Fungi (log_{10} CFU/mL)	Actinomycetes (log_{10} CFU/mL)
Control	5.17[a]	2.02[b]	5.01[a]
SNP	5.12[a]	2.02[b]	5.01[a]
AS	5.18[a]	2.14[a]	5.02[a]
AS + SNP	5.14[a]	2.09[b]	5.02[a]

2.7. Effect on native microflora of soil

2.7.1. Count of heterogeneous microbial population and soil properties

Microflora associated with soil samples was determined by the culture enrichment and serial dilution techniques (Mishra and Nautiyal, 2009). Heterogeneous soil population was counted on nutrient agar, Kenknight and Munaier's medium and Rose Bengal Chloramphenicol agar for bacteria, actinomycetes and fungi, respectively. pH and electric conductivity (EC) of soil samples were also measured (H1 2215 pH/ORP meter, Hanna instruments, USA; Orion, Thermo electron corporation, USA).

2.7.2. Soil enzyme activities

Soil enzyme activities were measured following the protocols of Kumari et al. (2017d).

2.7.2.1. Dehydrogenase. Dehydrogenase activity was measured spectrophotometrically using characteristics of TTC (2,3,5-triphenyltetrazolium chloride) reduction to TPF (triphenylformazan) as described by Mishra and Nautiyal (2009). Briefly, 5 g of soil was mixed with 5 mL of TTC solution prepared in 100 mM of tris-HCl (pH 7.7) and incubated at 28 °C for 24 h in the dark, on a shaker at 100 rpm. 5 ml of tris- HCl without TTC served as control. After incubation, 40 mL of acetone was added to each tube and further incubated at room temperature for 2 h in the dark with shaking every 10 min. 3 mL of supernatant was removed, centrifuged and absorbance was measured at 540 nm. Blank was prepared by adding 5 mL of tris buffer without addition of TTC to the soil sample. Dehydrogenase activity was expressed in micrograms of formazan per gram of sample (μg TPF/g dry wt/h).

2.7.2.2. Acid and alkaline phosphatase. Phosphatase activity was measured spectrophotometrically based on the determination of p-nitrophenol released after the incubation of soil with p-nitrophenyl phosphate for 1 h at 37 °C (Tabatabai, 1994). Briefly, 1 g of soil was mixed with 0.25 mL toluene, 4 ml MUB (pH 6.5 for the assay of acid phosphatase, pH 11.0 for the assay of alkaline phosphatase), and 1 mL of p-nitrophenyl phosphate solution (15 mM) made in the same buffer. The content was mixed and incubated at 37 °C for one hour, after which 1 mL of 0.5 M $CaCl_2$ and 4 mL of 0.5 M NaOH was added to it. The blank was prepared by adding one ml of p-nitrophenyl phosphate, after addition of 1 mL of 0.5 M $CaCl_2$ and 4 ml of 0.5 M NaOH immediately before the filtration of soil suspension. The soil suspension was mixed and filtered through Whatman no. 2 filter paper. The absorbance was recorded at 400 nm in triplicate and activity was expressed as μg of PNP/g dry wt/h.

2.7.2.3. β glucosidase. β glucosidase activity was measured spectrophotometrically using p-Nitrophenyl- β-D-glucoside (PNG) as substrate (Tabatabai, 1994). Briefly, 1 g of soil was mixed with 0.25 mL toluene, 4 mL MUB (pH 6.0) and 1 mL of PNG (25 mM) solution made in the same buffer. The content was mixed and incubated at 37 °C for 1 h. After which 1 mL of 0.5 M $CaCl_2$ and 4 ml of tris buffer (pH 12) was added to it. The soil suspension was mixed and filtered through Whatman no. 2 filter paper. The absorbance was recorded at 400 nm in triplicate and activity was expressed in μg of PNP/g dry wt/h.

2.7.2.4. Urease. Urease activity was measured using the protocols of Kandeler and Gerber (1988). The procedure was based on spectrophotometric determination of ammonia after incubation of the soil samples with urea solution. 5 g of moist soil was placed in Erlenmeyer flask, urea solution (2.5 M) was added to it, and incubated for 2 h at 37 °C. After incubation 50 mL of KCl solution was added and it was put on a shaker for 30 min. Blank was prepared by replacing urea with same volume of MQ. The solution was then filtered and the filtrate was analyzed for ammonium content using a spectrophotometer at 690 nm and activity was expressed as μg of NH_4/g dry wt/h.

2.7.2.5. Protease. Protease activity was determined through the method described by Ladd and Butler (1972). Tyrosine (Tyr) amino acid concentration was obtained in the soil samples after incubation with sodium caseinate. 1 g of moist soil was mixed with 5 mL tris buffer and 5 mL sodium caseinate solution. The mixture was incubated at 50 °C for 2 h on a shaking water bath. After incubation, 5 mL of TCA solution was added to it and mixed thoroughly. Resulting soil suspension was centrifuged and 5 mL of supernatant was mixed with 7.5 ml of the alkaline reagent. Blank was prepared by adding 5 mL sodium caseinate solution at the end of incubation and immediately before addition of TCA solution. After 15 min of incubation at room temperature, absorbance was recorded at 700 nm and activity was expressed in μg Tyr g^{-1} soil h^{-1}.

2.8. Microbial diversity using carbon source utilization pattern

To determine the difference in the carbon source utilization pattern of soil samples under different conditions Biolog Eco plates (Biolog, Inc., Hayward, CA, USA) were used (Mishra and Nautiyal, 2009). One gram of Soil sample was mixed with 99 mL of sterile 0.85% saline MQ water and put on rotary shaker for 60 min. Further, 150 μL of sample were inoculated in each well of Biolog Eco plates and incubated at 30 °C and data was recorded spectrophotometrically for day 1–7 at 590 nm. The rate of utilization of carbon source was indicated by the reduction of tetrazolium, a redox indicator dye, which changes from colourless to purple. Average well colour development (AWCD), indicative of microbial carbon source utilization was determined.

2.9. Statistical analysis

The results were displayed as means ± SD (± standard deviation). For statistical significance, means ± SD of all groups were compared and analysis of variance (ANOVA) was performed using a statistical package, SPSS 16.0 (SPSS Inc., Chicago, IL, USA). A probability of P-value of ≤ 0.05 was taken to indicate statistical significance. Further, Duncan's Multiple Range Test (DMRT) was used to identify the pairs of groups where the means are significantly different at $\alpha = 0.05$.

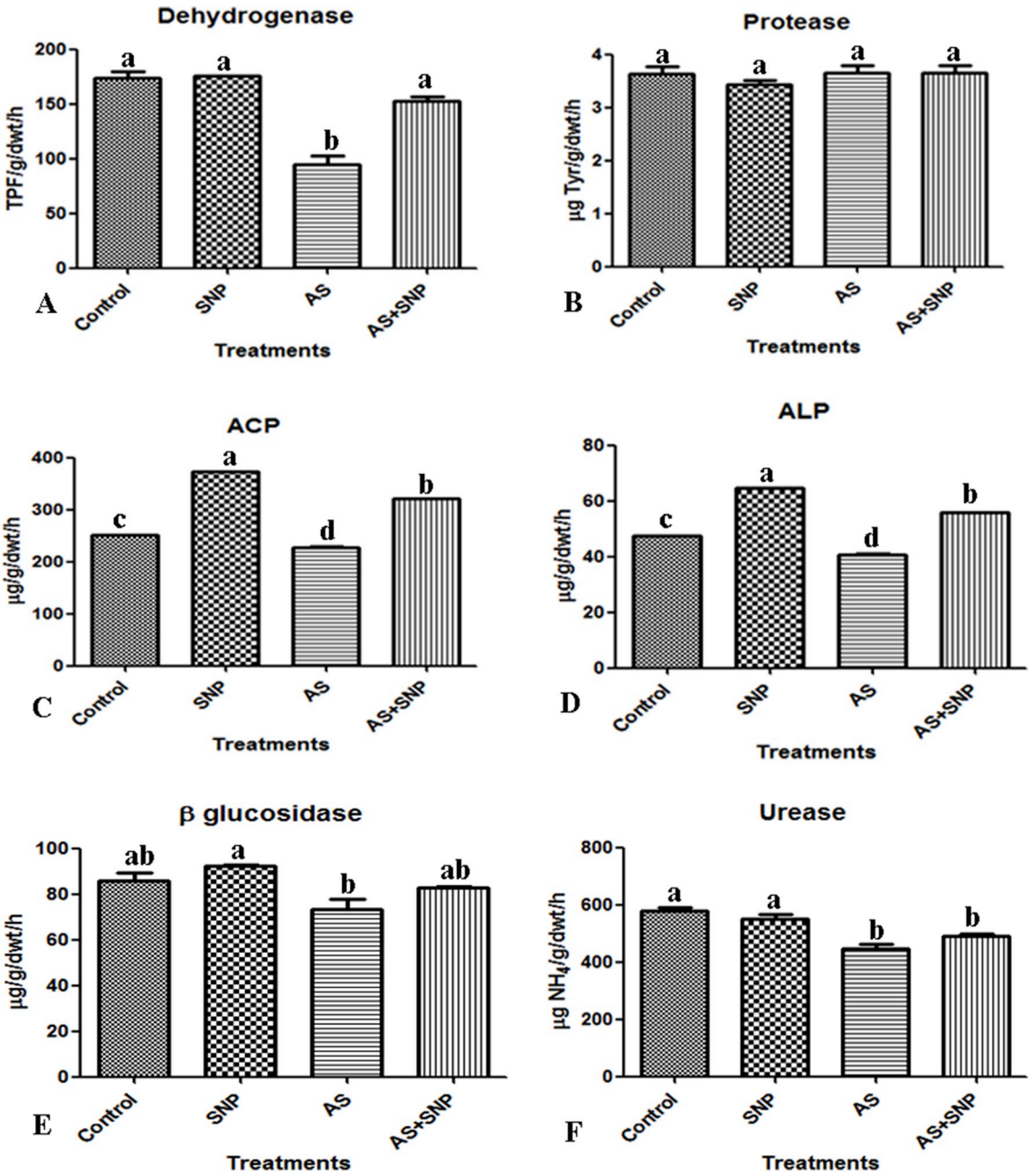

Fig. 7. Soil enzyme activities during harvesting of plants **(a)** dehydrogenase **(b)** protease **(c)** acid phosphatise (ACP) **(d)** Alkaline phosphatise (ALP) **(e)** β-glucosidase **(f)** urease. Values are the means of three replicates. Means sharing different alphabets "a", "b" differ significantly from each other at $p \leq 0.05$.

3. Result and discussions

3.1. Antagonistic effect of SNP against A. solani

A consistent concentration dependent decrease in biomass of *A. solani* was observed with SNP treatment. In broth assay, 100% decrease in spore count after day 3 of treatment and 73.3% decrease in fungal biomass after 7th day of treatment was observed (Fig. 1a,b). Silver nanoparticles have shown their antifungal activities against some *Alternaria* sp. (Rai et al., 2012). The particles used in this investigation possess higher antimicrobial activities as compared to their chemical counterparts because of surface coating of secondary metabolites of *T. viride* and their precise shape and size (Spherical, 2–5 nm) (Kumari et al., 2017b,c).

3.2. Detached leaf assay

SNP was able to control the early blight disease on tomato as observed *in vitro* (Fig. 2). The lesion size decreased in plants treated with SNP as compared to AS alone. The necrotic area and number of spores also decreased in SNP treated leaves. Detached leaf assays are easy methods which generally mimic the whole plant responses during stress (Boydom et al., 2013). SNP with their various modes of actions not only restricted the growth of *A. solani* but also minimised the damage of plant leaves.

3.3. Plant growth parameters

A clear decrease in number of lesions and plant heath was observed visually (Fig. 3) after treatment of biosynthesized silver nanoparticles as compared to AS alone plants.

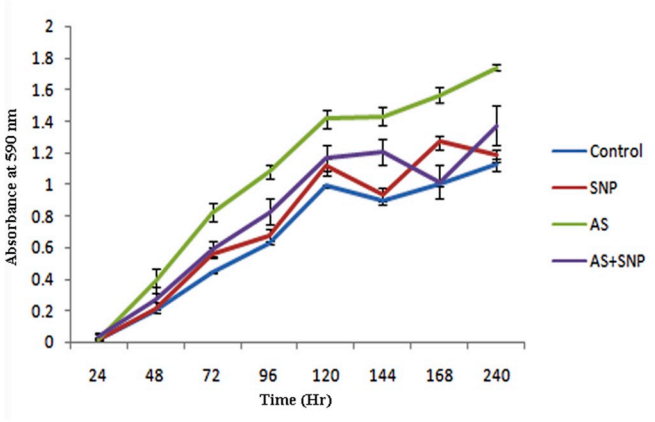

Fig. 8. Average well colour development (AWCD) during treatments of tomato leaves with SNP, AS + SNP and AS alone. (For interpretation of the references to colour in this figure legend, the reader is referred to the web version of this article.)

A significant increase of 32.58% was found in AS + SNP as compared to AS alone in fresh weight while dry weight of treated tomato plants non significantly increased to 23.42% as compared to AS alone plants (Fig. 4A,B). Spore count of *A. solani* reduced from 5.1* 10^5 spores/leaf to 1.05* 10^5 spores/leaf in AS + SNP treatment as compared to AS alone (Fig. 4C) indicating the potential of SNP as fungal growth inhibitor. Chlorophyll *a*, *b*, total chlorophyll and caretenoid contents were found lowest in plants affected with early blight disease while AS + SNP demonstrated a significant increase of 14.28, 50, 23.52 and 20% of chlorophyll *a*, *b*, total chlorophyll and caretenoid significantly as compared to AS alone (Fig. 4D).

Infection of *A. solani* clearly showed the symptoms of early blight disease including black lesions, necrotic zones and decreased growth parameters of tomato plants (Fig. 3b). The obvious symptoms were clearly diminished after application of SNP, making the plant as healthy as control in visual appearance (Fig. 3d). Ocsoy et al. (2013) have also supported the role of silver nanoparticles in amelioration of bacterial spot disease on tomato plants. Further, enhanced concentration of chlorophyll and caretenoids in AS + SNP can account for increased photosynthetic activities (Tripathi et al., 2017).

3.4. Assessment of stress markers

Concentrations of proline and LPX decreased by 38.59 and 30% in AS + SNP as compared to AS alone, while no significant difference was observed in content of proline and LPX in control and SNP alone (Fig. 5A, B). LPX depicts the peroxidation of lipid membrane of plant caused by ROS species while proline is a signalling molecule which is triggered by stress (Singh et al., 2013). Because of lesser invasion of *A. solani* inside the plant cells, TBARS substances were not produced, resulting in considerable decrease in LPX and proline.

3.5. Antioxidative activities of plants

Maximum phenolic content was found in SNP treated plants followed by AS + SNP treatment (Fig. 5C). Phenolic compounds are the major constituents of several anti-pathogenic compounds secreted by plants and serving as first line of defence. A significant decrease of 60 and 28.57% was observed in activities of PPO and SOD in AS + SNP treated plants in comparison to AS infected plants (Fig. 6B,C). A non significant increase of 23.52% and 31.42% was observed in activities of PAL and APX while activity of GoPX decreased 55% in AS + SNP as compared to AS alone (Fig. 6A, D, E). Antioxidant enzymes are redox based biomarkers which are all connected in a network and reflects the status of a cell when it is undergoing stress (Yang and Lee, 2015). During biotic stress, initially during early phase of infection, there is an oxidative burst, production of phenolic compounds, which enhances the level of antioxidative enzymes (Torres et al., 2006). In this study, maximum enhancement in stress related enzymes was found in AS infected plants which depicts the biotic stress the host is facing. Biotic stress caused by *A. solani,* generated free radicals by cell membrane and caused chlorophyll damage. As a result, antioxidants enzymes elevated to ameliorate the biotic stress caused by *A. solani*. When SNP was applied to the tomato plants, there was a significant reduction in stress markers, resulting in healthier status of plants with reduced ROS production. Similar results were found by Singh et al. (2013) and Dixit et al., 2016 were application of biocontrol agent altered the oxidative status in plants to combat the pathogen attack.

A significant increase in oxidative enzymes was also observed when plants were pre-treated with SNP. SNP did not only attenuate the population of *A. solani* by the various means of killing, but it also prepared the plants to cope up with the further stress. Krishnaraj et al. (2012) has also found in his study that the lower concentration of silver nanoparticles may help in boosting immunity of *Bacopa monnieri*.

An attempt was made to decipher the mode of actions of biosynthesized SNP in the amelioration of early blight disease in tomato (Graphical abstract).

The first and most important mechanism employed by SNP is direct inhibition of phytopathogen and reducing their spore count (Ocsoy et al., 2013). With different modes of actions, SNP inhibited growth of *A. solani*, preventing plant to establish infection and combating the collateral damage. By selecting the most potent nanoparticles among different shapes and sizes and coating them with secondary metabolites of *T. viride* makes biosynthesized SNP more potent than their other counterparts (Kumari et al., 2017b,c). In the earlier studies, authors have found that biosynthesized nanoparticles of small size (2–5 nm) with coating of several organic acids and antifungal metabolites of *T. viride* served as better antimicrobial agents than chemically synthesized silver nanoparticles of similar shape and size.

Foliar application of biosynthesized silver nanoparticles increased the first line of defence in tomato plants as evident by increased phenolics production and increased production of antioxidative enzymes. The increased resistance acquired by plants prepares them to minimize the ROS production after pathogen attack and thus minimizing the stress enzymes activities in AS + SNP plants.

Table 3
Diversity/evenness indices of soil microflora of tomato plants under treatments of Control, plants sprayed with silver nanoparticles (SNP), *A. solani* infected plants (AS alone) and *A. solani* + SNP plants (AS + SNP). Values are the means of three replicates. Means sharing different alphabets "a", "b" differ significantly from each other at $p \leq 0.05$.

	Control	SNP	AS	AS + SNP
Shannon diversity index	3.13 ± 0.057^a	3.14 ± 0.012^a	3.12 ± 0.015^b	3.13 ± 0.035^a
Shannon evenness index	0.91 ± 0.002^a	0.92 ± 0.005^a	0.92 ± 0.002^a	0.91 ± 0.005^a
Simpson diversity index	0.92 ± 0.002^a	0.92 ± 0.001^a	0.89 ± 0.002^b	0.90 ± 0.002^{ab}
McIntosh diversity index	0.96 ± 0.006^a	0.96 ± 0.006^a	0.95 ± 0.008^a	0.95 ± 0.002^a
McIntosh evenness index	0.95 ± 0.005^a	0.95 ± 0.002^a	0.94 ± 0.007^b	0.95 ± 0.005^a

Treatment of SNP was able to ameliorate the photosynthetic machinery as evident by the increased chlorophyll level in AS + SNP, thereby providing energy requirements to plants to combat biotic stress. Similar report of alleviating Cr phytotoxicity by silicon nanoparticles on *Pisum sativum* has been reported by (Tripathi et al., 2017).

3.6. Effect of tripartite interaction of plant- A. solani-SNP on native microflora

Nanoparticles can emerge as an inevitable alternative for plant protection, which may lead to influx of particles into the soil (Gogos et al., 2016). In this study also, an in depth knowledge is required regarding the fate of native microflora when they interact with the nanoparticles coming from tripartite interaction of plant- *A. solani*-SNP.

3.6.1. Count of heterogeneous microbial population and soil properties

The soil microbial population of bacteria, fungi and actinomycetes remained unchanged before and after treatment of silver nanoparticles (Table 1). Population of heterogeneous microbial population in rhizospheric soil directly indicates the health of soil (Pallavi et al., 2016).

Soil properties such as pH and electric conductivity of soil also remained unaffected in SNP treated soil, though EC in fungal infected soil increased significantly (Table 2). pH and electric conductivity are two the important factors of soil health, change of which directly effects the native microbial population. Change in EC of infected soil indicates deterioration in soil health, where as SNP treated soil was as healthy as control.

3.6.2. Soil enzymes

To assess the effect of SNP applied on plants, on native microflora of soil, dehydrogenase, acid and alkaline phosphatise, protease, β glucosidase and urease was estimated. There was no significant difference in activities of dehydrogenase, protease and urease in case of SNP treated plants when compared with control (Fig. 7). Plants affected with early blight disease showed considerable decrease of 52.94, 5, 11.1, and 12% respectively in activities of dehydrogenase, acid phosphatase, alkaline phosphatase, and urease in comparison to control while a non significant decrease was observed in β-glucosidase activity (Fig. 7A, C, D, E, F). There was no significant difference in activity of protease in AS treated plants in comparison to control (Fig. 7B). The activities of dehydrogenase, protease and β glucosidase of AS + SNP were comparable to control plants. AS + SNP treated plant showed 33.33 and 22.27% increase in activities of acid and alkaline phosphatase as compared to AS infected plants. The increase in phosphatase activities in AS + SNP might be a result of decreased population of *A. solani*. Eichler et al. (2004) also found decreased phosphates activity after fungal treatment of *Penicillium bilaii*.

Soil enzymes are the indirect markers of soil health (Baruah et al., 2017). A consistent decrease in dehydrogenase, phosphatise, β-glucosidase and urease activities were observed in fungus infected soil. Pathogens have the capability to alter the redox activity of plants by nutrient leaching (Fatima and Kumar, 2015) resulting in altered soil enzyme activity.

3.6.3. Biolog

Biolog provides the microbial fingerprint of a particular niche based upon the carbon source utilization pattern (Garland, 1996). It has been exploited to study bioremediation, plant-microbe interactions and microbial community from different spheres of Earth (Garland, 1996; Khan et al., 2012; Baruah et al., 2017). The average well colour development (AWCD) based upon the carbon source utilization depicted the similar AWCD pattern for control and SNP while the pattern was completely different in AS infected plants (Fig. 8). AWCD pattern for AS + SNP showed higher resemblance to SNP than AS infected plants. Further, diversity and evenness indices were calculated based upon the carbon source utilization pattern in different treatments (Kumari et al., 2017d). No significant differences among control, SNP and AS + SNP were observed for the samples collected using the McIntosh, Shannon, and Simpson indices, however AS alone soil showed a significant difference in Shannon and Simpson diversity indices and McIntosh evenness index (Table 3). The study clearly depicted the anti-pathogenic role of SNP without hampering the native soil microbial diversity.

4. Conclusions

An eco-friendly approach to combat early blight disease in tomato without hampering the health of native soil microflora was highlighted using potent biosynthesized silver nanoparticles at 5 μg/mL concentration. The nanoparticles were able to diminish the pathogenic population of *A. solani* both *in vitro* and *in vivo* in a concentration dependent manner. The pre-treatment of particles on tomato leaves prevented the establishment of infection and increased the resistance of host plant by diminishing the biotic stress and increasing the antioxidant and chlorophyll content. This study provided the biochemical basis of defence employed by tomato plants during tripartite interaction of plant-pathogen and nanoparticles however an in-depth study of molecular mechanisms employed by host plants is highly desirable.

Conflicts of interest

The authors declare that they have no conflict of interest.

Contributions

The idea was conceived by CSN and AM. The work was done by MK, SP and AB. MK and SP wrote the manuscript. AM critically analyzed the manuscript.

Acknowledgements

We thank Mr. Sumit Yadav, CSIR-NBRI for his guidance in Biolog studies. This study was partially funded by network project of Council of Scientific and Industrial Research (CSIR) “Plant Microbe Soil Interactions BSC 117”. MK thanks CSIR for awarding Junior and Senior Research Fellowship (JRF and SRF) to her.

References

Arnon, D.I., 1949. Copper enzymes in isolated chloroplasts. Polyphenoloxidase in *Beta vulgaris*. Plant Physiol. 24, 1–15.

Baruah, R., Mishra, S.K., Kalita, D.J., Silla, Y., Chauhan, P.S., Singh, A.K., Boruah, H.P.D., 2017. Assessment of bacterial diversity associated with crude oil contaminated soil samples from Assam. Int. J. Env. Sci. Technol. 14, 2155–2172.

Bates, L., Waldren, R.P., Teare, I.D., 1973. Rapid determination of free proline for water-stress studies. Plant Soil 39, 205–207.

Beauchamp, C., Fridovich, I., 1971. Superoxide dismutase: improved assays and an assay applicable to acrylamide gels. Anal. Biochem. Rev. 44, 276–287.

Boydom, A., Dawit, W., Getaneh, W., 2013. Evaluation of detached leaf assay for assessing leaf rust (*Puccinia triticina* Eriks.) resistance in wheat. J. Plant Pathol. Microb. 4, 5.

Bradford, M.M., 1976. A rapid and sensitive method for the quantitation of microgram quantities of protein utilizing the principle of protein-dye binding. Anal. Biochem. 72, 248–254.

Dixit, R., Agarwal, L., Gupta, S., Kumar, M., Yadav, S., Chauhan, P.S., Nautiyal, C.S., 2016. Southern blight disease of tomato control by 1-aminocyclopropane-1-carboxylate (ACC) deaminase producing *Paenibacillus lentimorbus* B-30488. Plant Signal Behav. 11 (2), e1113363. https://doi.org/10.1080/15592324.2015.1113363.

Eichler, B., Caus, M., Schnug, E., Koppen, D., 2004. Soil acid and alkaline phosphatase activities in regulation to crop species and fungal treatment. Landbauforsch. Volkenrode 54, 1–5.

Fatima, U., Kumar, M.S., 2015. Plant and pathogen nutrient acquisition strategies. Front. Plant Sci. 6, 750.

Garland, J.L., 1996. Analytical approaches to the characterization of samples of microbial communities using patterns of potential C source utilization. Soil Biol. Biochem. 28, 213–221.

Gogos, A., Moll, J., Klingenfuss, F., Heijden, M., Irin, F., Green, M.J., Zenobi, R., Buchel, T.D., 2016. Vertical transport and plant uptake of nanoparticles in a soil mesocosm experiment. J. Nanobiotechnol. 14, 40.

Heath, R., Packer, L., 1968. Photoperoxidation in isolated chloroplasts. I. Kinetics and

stoichiometry of fatty acid per- oxidation. Arch. Biochem. Biophys. 196, 385–395.
Hemeda, H.M., Klein, B.P., 1990. Effects of naturally occurring antioxidants on peroxidase activity of vegetable extracts. J. Food Sci. 55, 184–185.
Jamshidi, Ghanati, 2016. Taxanes content and cytotoxicity of hazel cells extract after elicitation with silver nanoparticles. Plant Physiol. Biochem. 110, 178–184.
Javed, R., Usman, M., Yücesan, B., Zia, M., Gürel, K., 2017. Effect of zinc oxide (ZnO) nanoparticles on physiology and steviol glycosides production in micro-propagated shoots of *Stevia rebaudiana* Bertoni. Plant Physiol. Biochem. 110, 94–99.
Kandeler, E., Gerber, H., 1988. Short-term assay of soil urease activity using colorimetric determination of ammonium. Biol. Fert. Soils 6, 68–72.
Khan, N., Mishra, A., Nautiyal, C.S., 2012. *Paenibacillus lentimorbus* B-30488r controls early blight disease in tomato by inducing host resistance associated gene expression and inhibiting *Alternaria solani*. Biol. Control 62, 65–74.
Krishnaraj, C., Jagan, E.G., Ramachandran, R., Abirami, S.M., Mohan, N., Kalaichelvan, P.T., 2012. Effect of biologically synthesized silver nanoparticles on *Bacopa monnieri* (Linn.). Process Biochem. 47 (4), 651–658.
Kumari, M., Mishra, A., Pandey, S., Singh, S.P., Chaudhry, V., Mudiam, M.K.R., Shukla, S., Kakkar, P., Nautiyal, C.S., 2016. Physico- Chemical condition optimization during biosynthesis leads to development of improved and catalytically efficient gold nanoparticles. Sci. Rep. 6, 27575.
Kumari, M., Pandey, S., Nautiyal, C.S., Mishra, A., 2017a. Facile a facile way for the bacterial DNA transformation by biosynthesized gold nanoparticles. FEMS Microbiol. Lett. 364, fnx081. https://doi.org/10.1093/femsle/fnx081.
Kumari, M., Shukla, S., Pandey, S., Giri, V.P., Tripathi, T., Bhatia, A., Kakkar, P., Nautiyal, C.S., Mishra, A., 2017b. Enhanced cellular internalization: a bactericidal mechanism more relative to biogenic nanoparticles than chemical counterparts. ACS Appl. Mat. Interfaces 9, 4519–4533.
Kumari, M., Pandey, S., Giri, V.P., Bhattacharya, A., Shukla, R., Nautiyal, C.S., Mishra, A., 2017c. Tailoring shape and size of biogenic silver nanoparticles to enhance antimicrobial efficacy against MDR bacteria. Microb. Pathog. 105, 346–355.
Kumari, M., Pandey, S., Mishra, S.K., Nautiyal, C.S., Mishra, A., 2017d. Effect of biosynthesized silver nanoparticles on native soil microflora via plant transport during plant-pathogen-nanoparticles interaction. 3 Biotech. 7 (5), 345.
Ladd, J.N., Butler, J.H.A., 1972. Short-term assays of soil proteolytic enzyme activities using proteins and dipeptide derivatives as substrates. Soil Biol. Biochem. 4, 19–30.
Lavania, M., Chauhan, P.S., Chauhan, S.V.S., Singh, H.B., Nautiyal, C.S., 2006. Induction of plant defence enzymes and phenolics by treatment with plant growth-promoting rhizobacteria *Serratia marcescens* NBRI1213. Curr. Microbiol. 52, 363–368.
Mallick, C.P., Singh, M.B., 1980. Plant Enzymology and Histoenzymology. Kalyani publishers, New Delhi, pp. 286.
Mishra, A., Kumari, M., Pandey, S., Chaudhry, V., Gupta, K.C., Nautiyal, C.S., 2014. Biocatalytic and antimicrobial activities of gold nanoparticles synthesized by Trichoderma sp. Bioresour. Technol. 166, 235–242.
Mishra, A., Nautiyal, C.S., 2009. Functional diversity of the microbial community in the rhizopshere of chickpea grown in diesel fuel-spiked soil amended with *Trichoderma ressei* using sole-carbon-source utilization profiles. World J. Microbiol. Biotechnol. 25, 1175–1180.
Mishra, S., Srivastava, S., Tripathi, R.D., Govidarajan, R., Kuriakose, S.V., Prasad, M.N.V., 2006. Phytochelatin synthesis and response of antioxidants during cadmium stress in *Bacopa monnieri* L. Plant Physiol. Biochem. 44, 25–37.
Ocsoy, I., Paret, M.L., Ocsoy, M.A., Kunwar, S., Chen, T., You, M., Tan, W., 2013. Nanotechnology in plant disease management: DNA-directed silver nanoparticles on graphene oxide as an antibacterial against *Xanthomonas perforans*. ACS Nano 7 (10), 8972–8980.
Pallavi, Mehta, C.M., Srivastava, R., Arora, S., Sharma, A.K., 2016. Impact assessment of silver nanoparticles on plant growth and soil bacterial diversity. 3 Biotech 6, 254.
Rai, M.K., Deshmukh, S.D., Ingle, A.P., Gade, A.K., 2012. Silver nanoparticles: the powerful nanoweapon against multidrug-resistant bacteria. J. Appl. Microbiol. 112, 841–852.
Singh, A., Sarma, B.K., Upadhyay, R.S., Singh, H.B., 2013. Compatible rhizosphere microbes mediated alleviation of biotic stress in chickpea through enhanced antioxidant and phenylpropanoid activities. Microbiol. Res. 168, 33–40.
Tabatabai, M.A., 1994. Soil enzymes. In: Mickelson, S.H., Bigham, J.M. (Eds.), Methods of Soil Analysis, Part 2. Microbiological and Biochemical Properties. SSSA, Madison, Wis.
Torres, M.A., Jones, J.D.G., Dang, J.L., 2006. Reactive oxygen species signalling in response to pathogen. Plant Physiol. 141, 373–378.
Tripathi, D.K., Singh, S., Singh, V.P., Prasad, S.M., Dubey, N.K., Chauhan, D.K., 2017. Silicon nanoparticles more effectively alleviated UV-B stress than silicon in wheat (*Triticum aestivum*) seedlings. Plant Physiol. Biochem. 110, 70–81.
Tripathi, D.K., Singh, V.P., Prasad, S.M., Chauhan, D.K., Dubey, N.K., 2015. Silicon nanoparticles (SiNp) alleviate chromium (VI) phytotoxicity in *Pisum sativum* (L.) seedlings. Plant Physiol. Biochem. 96, 189–198.
Wang, H., Thorling, C.A., Liang, A., Bridle, K.R., Grice, J.E., Zhu, Y., Crawford, D.H.G., Xu, Z.P., Liu, X., Roberts, M.S., 2015. Diagnostic imaging and therapeutic application of nanoparticles targeting the liver. J. Mater. Chem. B 3, 939–958.
Wang, P., Menzies, N.W., Dennis, P.G., Guo, J., Forstner, C., Sekine, R., Lombi, E., Kappen, P., Bertsch, P.M., Kopittke, P.M., 2016. Silver nanoparticles entering soils via the wastewater–sludge–soil pathway pose low risk to plants but elevated Cl concentrations increase Ag bioavailability. Environ. Sci. Technol. 50, 8274–8281.
Yang, H.Y., Lee, T.H., 2015. Antioxidant enzymes as redox-based biomarkers: a brief review. BMB Rep. 48 (4), 200–208.